Permeability of Dimyristoyl Phosphatidylcholine/Dipalmitoyl Phosphatidylcholine Bilayer Membranes with Coexisting Gel and Liquid-Crystalline Phases

Stéphane G. Clerc and Thomas E. Thompson
Department of Biochemistry, University of Virginia, Charlottesville, Virginia 22908 USA

ABSTRACT The passive permeation of glucose and a small zwitterionic molecule, methyl-phosphoethanolamine, across two-component phospholipid bilayers (dimyristoyl phosphatidylcholine (DMPC)/dipalmitoyl phosphatidylcholine (DPPC) mixtures) exhibit a maximum when gel domains and fluid domains coexist. The permeability data of the two-phase bilayers cannot be fitted to single-rate kinetics, but are consistent with a Gaussian distribution of rate constants. In pure DMPC and DPPC as well as in their mixtures, at the temperature of the maximum excess heat capacity, the logarithm of the average permeability rate constants are linearly correlated with the mole fraction of DPPC in the total system. In addition, in the 50:50 mixture, the excess heat capacity values as well as the apparent fractions of interfacial lipid correlate with the logarithm of the excess permeabilities in the two-phase region. These results suggest that small polar molecules can cross the membrane at the interface between gel and fluid domains at a much faster rate than through the homogeneous phases; the acyl chains located at the domain interface experience lateral density fluctuations that are inversely proportional to their average length, and large enough to allow rapid transmembrane diffusion of the solute molecules. The distribution of the permeability rate constants may reflect temporal and spatial fluctuations of the lipid composition at the phase boundaries.

INTRODUCTION

It has been known for some time that the permeability of one-component phospholipid bilayers to small water-soluble molecules may be larger at the temperature of the main phase transition (T_m) than when the bilayers are either all-gel or all-fluid at temperatures near T_m (Papahadjopoulos et al., 1973; Blok et al., 1975; Marsh et al., 1976; Van Hoogevest et al., 1984; El-Mashak and Tsong, 1985; Georgallas et al., 1987; Bramhall et al., 1987). The magnitude of the increase is strongly dependent on both the solute and the type of liposomes used. For example, dipalmitoyl phosphatidylcholine multilamellar vesicles have a maximum permeability for Na^+ and Rb^+ at T_m; but in dipalmitoyl phosphatidylcholine large unilamellar vesicles, this effect is less important for Na^+ and cannot be observed for Rb^+ (El-Mashak and Tsong, 1985). The efflux of 5/6-carboxyfluorescein from sonicated vesicles also reaches a local maximum at T_m, and the permeation rate at T_m is inversely dependent on the phospholipid acyl chain length ($C_{14} > C_{16} > C_{18} > C_{20}$) (Bramhall et al., 1987). The substantial increase of permeability has been attributed to fluctuations in the lateral compressibility of the bilayer at T_m (Linden et al., 1973; Doniach, 1978; Nagle and Scott, 1978; Georgallas et al., 1987) or to acyl chain packing mismatch at the interfacial region between gel and fluid domains (Papahadjopoulos et al., 1973; Marsh et al., 1976; Kanehisa and Tsong, 1978; Van Hoogevest et al., 1984). Theoretical model studies of the chain-melting phase transition of saturated phosphatidylcholines performed by Monte Carlo calculations (Cruzeiro-Hansson and Mouritsen, 1988; Ipsen et al., 1990) show that gel-fluid domain boundary lengths are at a maximum at T_m. These simulations suggest that the lipid molecules at the domain interfaces are subject to lateral density fluctuations, which are inversely proportional to the acyl chain length, that cause the maximum in the bilayer permeability at T_m.

In this study, the passive permeation of glucose and of a small zwitterionic molecule, methyl-phosphoethanolamine, has been investigated across phospholipid bilayers composed of mixtures of dimyristoyl phosphatidylcholine and dipalmitoyl phosphatidylcholine. For each composition, the permeability coefficients for these solutes exhibit a maximum in the coexistence region of gel and fluid domains. The experimental data show that the coexistence of phase domains leads to a deviation from single-exponential permeation kinetics. In addition, the logarithms of the permeability coefficients of two-component, two-phase bilayers are shown to be proportional to the mole fraction of DPPC in the total system. The logarithms of the permeability coefficients are also proportional to the apparent fraction of lipids at the solid/fluid interface. These results suggest that the permeability at the domain interface is the result of lateral density fluctuations that increase the probability of defect formation and the average free volume in the acyl chain region.

MATERIALS AND METHODS

Dimyristoyl phosphatidylcholine (DMPC) and dipalmitoyl phosphatidylcholine (DPPC) were purchased from Avanti Polar Lipids (Alabaster, AL)

Received for publication 25 April 1994 and in final form 13 March 1995.

Address reprint requests to Dr. Thomas E. Thompson, Department of Biochemistry, University of Virginia School of Medicine, Box 440, Charlottesville, VA 22908. Tel.: 804-924-5139; Fax: 804-924-5069; E-mail: tet@virginia.edu.

Abbreviations used: DMPC, 1,2-dimyristoyl-*sn*-glycero-3-phosphocholine; DPPC, 1,2-palmitoyl-*sn*-glycero-3-phosphocholine; LUV, large unilamellar vesicles; TLC, thin layer chromatography; MPE, methyl-2-aminoethyl hydrogen phosphate; T_m, main phase transition; PIPES, piperazine-*N*-*N*′-bis (ethanesulfonic acid); EDTA, ethylenediaminetetraacetic acid.

0006-3495/95/06/2333/09 $2.00

and kept stored under N_2 at −20°C. Phosphorous oxychloride and tetrahydrofuran were purchased from Aldrich (Milwaukee, WI). Triethylamine, PIPES and D-glucose were purchased from Sigma Chemical Co. (St. Louis, MO). Ethanolamine, carbon tetrachloride, acetic acid, and ammonia were purchased from Fisher Scientific (Fair Lawn, NJ). Methanol was obtained from EM Sciences (Gibbstown, NJ). Dichloromethane was obtained from Mallinckrodt (St. Louis, MO). Sephadex G-50 was purchased from Pharmacia (Uppsala, Sweden). [^{14}C]methanol (42 mCi/mmol) was purchased from ICN Biomedical (Irvine, CA). [^{14}C]-D-glucose (3 mCi/mmol) was purchased from Amersham (Arlington Heights, IL). [^{3}H]cholesteryl oleate (82.0 Ci/mmol) was purchased from DuPont NEN (Boston, MA). Phospholipids were routinely assayed using either a phosphate assay (Bartlett, 1959) or an ammonium ferrothiocyanate assay (Stewart, 1980).

Synthesis of methyl-phosphoethanolamine

The structure of the methyl-phosphoethanolamine (MPE) molecule is shown in Fig. 1. The method originally developed by Eibl (1978) for phospholipids was slightly modified because of the hydrophilic character of the products. To maintain anhydrous conditions, the glassware was dried overnight at 130°C, assembled while warm, and flushed with dried N_2 gas. Methanol (30 mmol) and triethylamine (30 mmol) in carbon tetrachloride (50 ml) was added dropwise under anhydrous conditions over a period of 1 h to a stirred solution of phosphorous oxychloride (30 mmol) in carbon tetrachloride (50 ml) at 0°C (ice bath). The mixture was stirred at 0°C for 2 h. Ethanolamine (30 mmol) and triethylamine (60 mmol) in dichloromethane (50 ml) were then added dropwise under anhydrous conditions over a period of 1 h to the stirred reaction mixture at 0°C. Stirring was continued overnight at 10°C (cold room). The mixture was allowed to warm to room temperature and was then filtered under vacuum to remove the precipitated triethylamine hydrochloride. The solvent was removed by rotary evaporation under reduced pressure, and the solid residue was dissolved in tetrahydrofuran (50 ml) to precipitate the remaining triethylamine hydrochloride. After filtration, the tetrahydrofuran was rotary evaporated to yield the cyclic intermediate as a yellow oil. The purity was checked by thin layer chromatography (TLC) on silica gel GHL plates, eluting with acetone (R_f = 0.4). The intermediate was dissolved in tetrahydrofuran (25 ml) and 20% (v/v) aqueous acetic acid (50 ml) at 0°C, and the reaction mixture was stirred for 2 h at room temperature. The solvents were removed by rotary evaporation under reduced pressure, and the resulting oily residue dissolved in methanol (50 ml) to precipitate the crude product. Purification was achieved by column chromatography (30 × 2.4 cm) using silica gel 60 (70–230 mesh, EM laboratories) and eluting with methanol/5% aqueous ammonia (100:15) (v/v). The product was detected in the fractions by TLC on silica gel GHL plates using the same solvent (R_f = 0.48). The fractions containing the pure product were pooled. Concentration by rotary evaporation and overnight lyophilization gave the pure products as white solids. The final yields for purified products was 62%.

Synthesis of [^{14}C]MPE

[^{14}C]methanol (4.8 μmol, 200 μCi) in carbon tetrachloride (500 μl) was added to a stirred solution of phosphorous oxychloride (25 μmol) in carbon tetrachloride (50 μl) maintained at 0°C. Then, methanol (20 μmol) and triethylamine (25 μmol) in carbon tetrachloride (50 μl) were added. The mixture was stirred for 1 h at room temperature. Ethanolamine (26 μmol) and triethylamine (60 μmol) in dichloromethane (50 μl) were added at room temperature, and the mixture was stirred for 2 h. The solvents were evaporated under a stream of N_2 to yield the crude radioactive product. Purification was achieved by preparative TLC on silica gel G eluting with methanol/5% aqueous ammonia (100:15) (v/v).

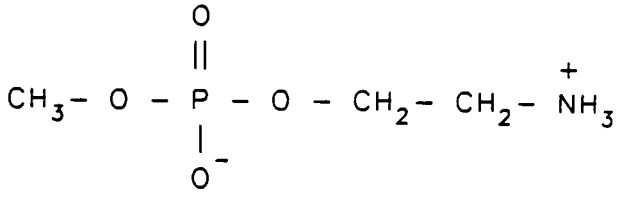

FIGURE 1 Structure of methyl-phosphoethanolamine (MPE, methyl 2-aminoethyl hydrogen phosphate).

Preparation of extruded vesicles

Dispersions in aqueous buffer of large unilamellar vesicles (LUV) were made by extrusion (Hope et al., 1985). The lipids and the radioactive markers were dissolved in chloroform and dried by rotary evaporation under reduced pressure at 40°C to obtain a uniform thin film. Any residual solvent was removed by overnight lyophilization. The dried lipids and the appropriate buffer were warmed at a temperature above the phase transition temperature of the lipids; then the buffer was added to the lipids, and a suspension of multilamellar vesicles was formed by gently agitating the flask. The suspension was frozen at −60°C in a bath of refrigerated methanol and thawed at 50°C in a water bath; the freeze-thaw cycle was repeated 5 times. Extrusion was performed 15 times through two stacked 0.1 μm pore diameter polycarbonate filters obtained from Nucleopore (Pleasanton, CA) using the pressure device built by Lipex Biomembrane (Vancouver, BC, Canada). The pressure was obtained with compressed N_2 gas, and the vesicle suspensions were routinely extruded at 2000 kPa. The apparatus was maintained in a water bath at a temperature above the phase transition temperature of the lipids. The size distribution of the vesicles was determined by dynamic light scattering with a Nicomp model HN5–90 instrument and a Nicomp model 170 autocorrelator (Nicomp, Goleta, CA). The mean vesicle diameters were close to 100 nm with SDs of about 30 nm. Vesicle suspensions were always diluted to a low lipid concentration (1 mM).

Calorimetry

LUV composed of DMPC/DPPC mixtures (70:30, 50:50, or 30:70 (mol/mol)) were prepared in the following buffer: 50 mM KCl, 10 mM PIPES, 1 mM EDTA, 3.1 mM NaN_3 (0.02%), pH 7.0. The heat capacity curves of these lipid mixtures were obtained by differential scanning calorimetry on a Hart Scientific (Pleasant Grove, UT) model 7707 microcalorimeter. The scan rate was 10°C/h, both in the heating mode and in the cooling mode. The samples were equilibrated by scanning twice from 10 to 55°C and back to 10°C; the data were then collected in the heating mode. A baseline scan was collected using buffer only and was subtracted from the lipid heat capacity curves.

The overall enthalpy changes associated with the transition were calculated by integrating the excess heat capacity curves, C_p:

$$\Delta H = \int_{T_0}^{T_n} C_p(t)\, dt \tag{1}$$

between temperatures at which the phospholipids are in the gel state (T_0) or in the liquid-crystalline state (T_n). The numerical integrations were carried out using the trapezoidal rule. The fractional melting $F_f(T)$ at temperature T, i.e., the fraction of phospholipid molecules in the liquid-crystalline state, was approximated by (Freire and Biltonen, 1978):

$$F_f(T) = \frac{\Delta H(T)}{\Delta H}, \tag{2}$$

where

$$\Delta H(T) = \int_{T_0}^{T} C_p(t)\, dt. \tag{3}$$

Although the theory for thermal transitions developed by Freire and Biltonen (1978) is strictly valid only for one-component systems, it was used as an approximation with DMPC/DPPC mixture data to estimate the ap-

parent fraction of phospholipid molecules at the gel-fluid boundary, F_{fg}:

$$F_{fg} = \frac{4F_f(\langle l_f\rangle^{1/2} + 1)}{(\langle l_f\rangle^{1/2} + 2)^2}. \quad (4)$$

$\langle l_f\rangle$, the average size of a fluid cluster, was calculated as

$$\langle l_f\rangle = \frac{z}{z-1} \quad (5)$$

The residual partition function z at temperature T was computed by numerical integration:

$$z = \exp\left[\int_T^{T_n} \frac{\Delta H - \Delta H(T)}{RT^2}\,dT\right]. \quad (6)$$

Permeability experiments

LUV (100 mM lipids) containing a radioactive, nonexchangeable marker ([^{3}H]cholesteryl oleate) and [^{14}C]MPE were prepared by extrusion in the following buffer: 5 mM MPE, 10 mM NaH_2PO_4/Na_2HPO_4, 40 mM NaCl, 1 mM EDTA, 3.1 mM NaN_3, pH 7.0. The vesicles were purified from the untrapped radioactive solute by gel exclusion chromatography on a Sephadex G-50 column (20 × 0.6 cm) at room temperature using the same buffer as the one used to prepare the vesicles. The nonspecific adsorption of phospholipids was minimized by loading the column with 50:50 DMPC/DPPC LUV to saturate the gels with phosphatidylcholine. The fractions containing the vesicles were pooled (0.9 ml, ~10 mM lipid) in 1 ml micro-reaction vials and incubated under argon at the experimental temperature in a Neslab (Newington, NH) water bath model RTE-110. The temperature control was accurate to about ±0.15°C. At different time intervals, the amount of radioactive solute present in the vesicles was measured by separating the vesicles from the external medium by gel exclusion chromatography. Aliquots (20 μl) were removed from the incubation vial and run on Sephadex G-50 spin mini-column (V_t = 1.5 ml) at room temperature using a table top International Clinical Centrifuge (Boston, MA) at full speed for 30 s. The ^{3}H and ^{14}C radioactivity in the eluant were measured by liquid scintillation counting and corrected for the background radiation levels. The amount of trapped radioactive solute at time t, q_t, was normalized as follows:

$$\frac{q_t}{q_0} = \frac{^{14}C(t)\,/\,^3H(t)}{^{14}C(0)\,/\,^3H(0)}. \quad (7)$$

^{3}H and ^{14}C were determined in the vesicle fractions at zero time (0) and successive times (t) by liquid scintillation counting. The kinetic data were analyzed using nonlinear curve-fitting procedures such as the Nelder-Mead Simplex method and the Levenberg-Marquardt method (Press et al., 1986).

The experimental procedure described above is unsuitable for measuring permeability rate constants larger than 10 h^{-1} (half-time of permeation <5 min). Therefore, the permeability of MPE in pure DMPC vesicles was estimated using a water-jacketed Sephadex G-50 gel filtration column (20 × 0.6 cm). The amount of trapped solute was determined by gel filtration at 13°C, a temperature below the phase transition of DMPC. Then the temperature of the column was raised to the experimental temperature (23.5°C, the DMPC phase transition temperature), and 100 μl vesicle aliquots were run through the column. The incubation time was calculated as: $t = V/R$, where V is the column volume and R is the elution flow rate. By varying the flow rate of the eluting buffer (15, 33, and 51 ml/h), the incubation time was changed (2.5, 3.8, and 8.4 min). The ^{3}H and ^{14}C radioactivity in the vesicle fractions were measured as described above.

RESULTS

Calorimetry on DMPC/DPPC binary mixtures

The phase diagram obtained from differential scanning calorimetry with multilamellar vesicles (Mabrey and Sturtevant, 1976) is shown in Fig. 2. The diagram is divided into two uniform regions, the gel phase and the liquid-crystalline phase, in which the mixing of the two lipid species is close to ideal, and a two-phase region where DPPC-enriched gel phase domains coexist with DMPC-enriched liquid-crystalline phase domains. The diagram is that of an isomorphous mixture.

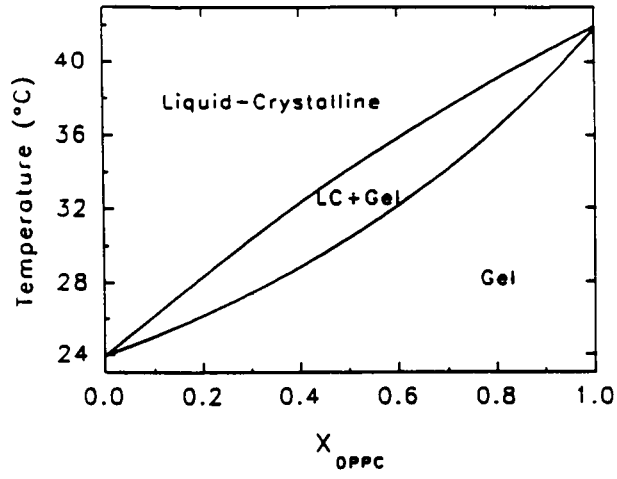

FIGURE 2 Equilibrium phase diagram for DMPC/DPPC (adapted from Mabrey and Sturtevant, 1976). This phase diagram was constructed from differential scanning calorimetry data obtained with multilamellar vesicles. The liquid-crystalline, gel and mixed phase region (LC + Gel) are indicated on the figure.

The excess heat capacity curves of extruded vesicles made of DMPC/DPPC, shown in Fig. 3, exhibit broad asymmetric transitions (width at half-height of ~3°C). The presence of a single peak for each scan suggests that the vesicle suspensions were homogeneous in composition. Therefore, it is likely that no separation of the lipid species occurred during the suspension of the dried lipids in the aqueous buffer or during the extrusion procedure. The onset and offset temperatures of the transitions are consistent with the DMPC/DPPC phase diagram. However, a slight shoulder at ~2.5°C below the main transition temperature was observed for each composition; such a distortion has been noted previously with extruded vesicles made of pure DPPC (Van Osdol et al., 1991). It may be the result of the morphology of the extruded vesicles, i.e., the inhomogeneities in the radii of curvature of the bilayers produced by the nonspherical shape of the vesicles.

Glucose permeability in 50:50 DMPC/DPPC vesicles

The kinetics of [^{14}C]glucose efflux from extruded vesicles composed of an equimolar mixture of DMPC and DPPC were studied at temperatures at which the bilayer was in the gel phase (24°C), in the liquid-crystalline phase (50°C), or in the mixed-phase region (33°C) (Fig. 4). The data for the uniform phases were fitted to single-exponential decays; the bilayers in the gel state were almost impermeable to glucose ($t_{1/2} \approx 10$ days), but the rate of permeation was increased by several orders of magnitudes when the bilayers were in the

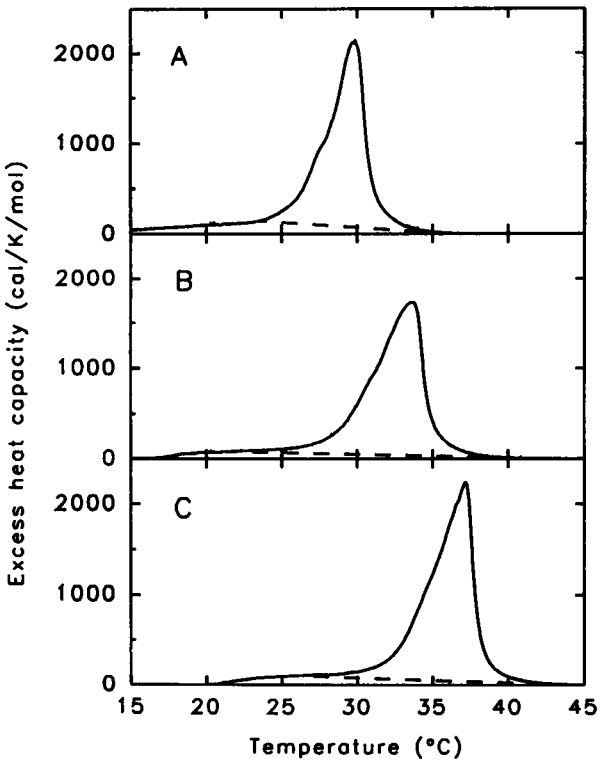

FIGURE 3 Excess heat capacity curves determined by differential scanning calorimetry of DMPC/DPPC LUV of 100 nm diameter made by extrusion in 50 mM KCl, 10 mM PIPES, 1 mM EDTA, 3.1 mM NaN_3 (0.02%), pH 7.0. The compositions are, from top to bottom: (*A*) 70:30, (*B*) 50:50, (*C*) 30:70 (mol/mol). The scan rate is 10°C/h in the heating mode. No correction has been made for the time response of the calorimeter. The dashed lines represent the linear baselines used for the integrations of the excess heat capacity functions.

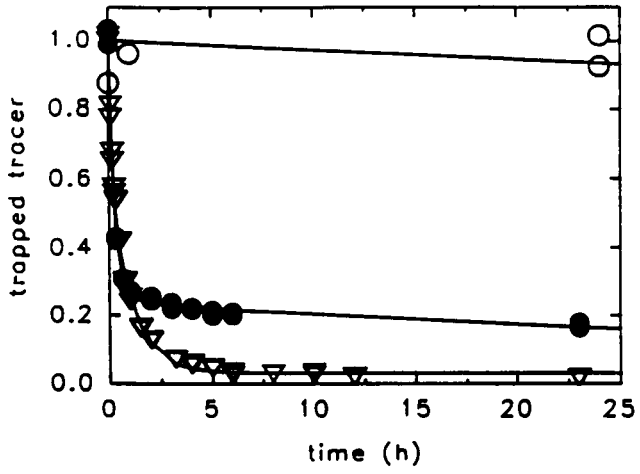

FIGURE 4 Glucose permeability kinetics in 50:50 (mol/mol) DMPC/DPPC LUV of 100 nm diameter in the gel phase at 24°C (○), the mixed phase at 33°C (▽), and the liquid-crystalline phase at 50°C (●). For experimental conditions, see text. The solid lines represent the best fits to a single-exponential decay (24 and 50°C) or to a double-exponential decay (33°C) plus a baseline. Buffer composition: 5 mM glucose, 10 mM NaH_2PO_4/Na_2HPO_4, 40 mM NaCl, 1 mM EDTA, 3.1 mM NaN_3, pH 7.0.

liquid-crystalline phase ($t_{1/2} \approx 10$ min). The 10% entrapment at equilibrium ($t = \infty$) for vesicles in the liquid-crystalline phase was higher than the 2% predicted from theoretical encapsulation considerations. The lipid concentration in the incubation medium was about 10 mM, and the theoretical aqueous phase entrapment capacity of spherical vesicles of 100 nm in diameter is 0.2%/mM lipid; therefore, 2% of the radioactive solute should be in the vesicles at equilibrium. This deviation was observed also for the permeation of glucose across palmitoyl-oleoylphosphatidylcholine bilayers in the fluid phase (data not shown). Thus, ~90% of the radioactive solute was able to diffuse across the membrane in the fluid phase, whereas the remaining 10% stayed associated with the vesicles over the course of the experiments. A similar observation was reported for the exchange of labeled DMPC between LUV made by extrusion and composed of DMPC (Wimley and Thompson, 1990). The origin of the excess of solute in the vesicle compartment is not understood.

The efflux of glucose for the temperature at which the two phases coexisted (33°C) was much faster than that expected if permeation occurred exclusively through the liquid-crystalline phase. From the fluid-phase rate at 50°C, assuming an activation energy of 27 kcal/mol and that half of the membrane area is fluid phase, the rate at 33°C should have been on the order of 0.25 h^{-1} ($t_{1/2} \approx 2.8$ h). Furthermore, the kinetics did not follow a single exponential decay, but the data could be fitted to the sum of two exponentials. About 65% of the radioactive solute left the vesicles with a half-time of about 17 min, and about 35% with a half-time of about 1.6 h. The inability to fit the data to a single-exponential decay was also observed with charged vesicles containing 1.75 mol% DMPG, with vesicles purified by gel filtration on a Sephacryl S-1000 column and with [^{3}H]glucose from ^{14}C-labeled vesicles (data not shown). In addition, the influx of glucose into 50:50 DMPC/DPPC vesicles at 33°C showed a similar deviation of the kinetics from a single-exponential decay (data not shown).

MPE permeability in DMPC/DPPC vesicles

As shown in Fig. 5, the kinetics of MPE efflux from 50:50 DMPC/DPPC vesicles exhibited a pattern similar to that of glucose permeability. The gel-state membranes were almost impermeable, the liquid-crystalline membranes exhibited faster permeability kinetics, and the membranes with coexisting phases were even more permeable than the membranes in the liquid-crystalline state. In addition, the mixed-phase data could not be fitted to single-exponential decays.

A correlation was observed between the two rate constants obtained from the double-exponential decay fits for the permeability data of different solutes in 50:50 DMPC/DPPC vesicles (Fig. 6 *A*) and for MPE in DMPC/DPPC vesicles of different compositions (Fig. 6 *B*). Therefore, the deviation of the permeability kinetics from a single-exponential decay had to reflect a property common to all of the systems studied, i.e., the coexistence of gel and the liquid-crystalline do-

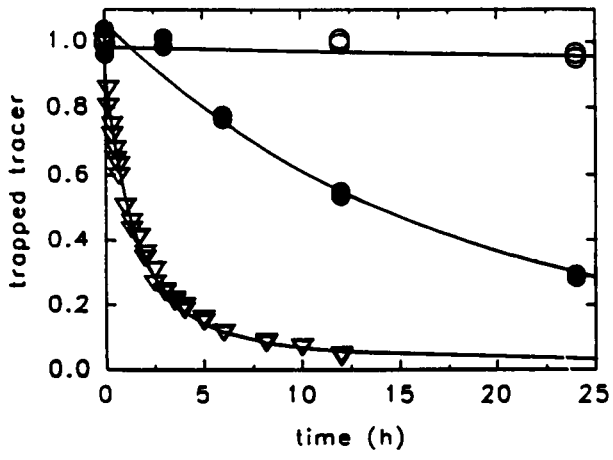

FIGURE 5 MPE permeability kinetics in 50:50 (mol/mol) DMPC/DPPC LUV of 100 nm diameter in the gel phase at 25°C (○), the mixed phase at 33°C (▽), and the liquid-crystalline phase at 50°C (●). For experimental conditions, see text. The solid lines represent the best fits to a single-exponential decay (25 and 50°C) or to a double-exponential decay (33°C) plus a baseline. Buffer composition: 5 mM MPE, 10 mM NaH_2PO_4/Na_2HPO_4, 40 mM NaCl, 1 mM EDTA, 3.1 mM NaN_3, pH 7.0.

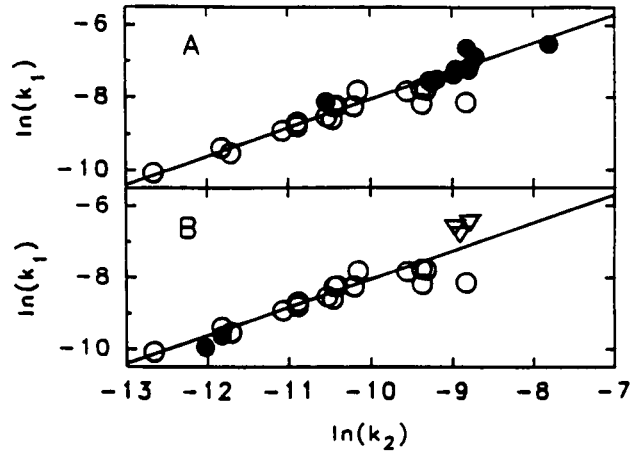

FIGURE 6 Permeability in DMPC/DPPC vesicles in the coexisting phase state, fitted to the sum of two exponential decays with rates k_1 and k_2 (s^{-1}). (*A*) Correlation of the logarithms of the two permeability rate constants of different solutes (MPE (○) and glucose (▼)) in 50:50 DMPC/DPPC vesicles. (*B*) Correlation of the logarithms of the two permeability rate constants of MPE in DMPC/DPPC LUV of different compositions (30:70 (●), 50:50 (○), and 70:30 (▽)). The solid line represents the best fit to a straight line of the combined data sets (*A* and *B*): $\ln(k_1) = 0.786\ (\pm 0.045) \times \ln(k_2) - 0.18\ (\pm 0.45)$.

mains in the vesicle membranes. In the Discussion, we propose the existence of a distribution of the permeability rate constants due to fluctuations within vesicles of the lipid composition at the boundaries between the gel-phase domains and the liquid-crystalline domains. If the rate constants are assumed to be distributed normally, then the permeability kinetics obtained with such vesicles can be fitted to the Laplace transform of the normal distribution (Eq. A.5 in the Appendix), and the average values of the rate constants can be estimated.

The permeability of MPE across 50:50 DMPC/DPPC membranes was studied at different experimental temperatures ranging from 25 to 50°C, i.e., with bilayers in the gel state, in the mixed-phase state, or in the liquid-crystalline phase (Fig. 7). The average rate constants plotted as a function of temperature exhibited a sharp maximum in the two-phase coexistence region.

The effect of the bilayer composition on the MPE permeability was investigated with vesicles made of pure DMPC, pure DPPC, or mixtures of the two lipid species (X_{DPPC} = 0.3, 0.5, or 0.7) at temperatures of maximal heat capacity, i.e., at temperatures at which the proportion of phospholipid molecules in the liquid-crystalline state was approximately equal to that in the gel state. The experimental results showed that DMPC membranes were more permeable than DPPC membranes and that, in the binary mixtures, the natural logarithms of the rate constants decreased linearly with the mole fraction of DPPC present in the bilayer (Fig. 8).

DISCUSSION

Distribution of the permeability rate constants

The kinetics of the permeation of tracer molecules across DMPC/DPPC bilayers with coexisting gel and fluid phases are not single-exponential decays. The experimental data can be fitted to the sum of two exponential decays, but the logarithms of the two rate constants are correlated, independently of either the permeant type (glucose or MPE) or the bilayer composition (X_{DPPC} = 0.3, 0.5, or 0.7, Fig. 6). Therefore, the complexity of the efflux kinetics is not due to experimental artifacts, but is the result of the particular structure of the lipid

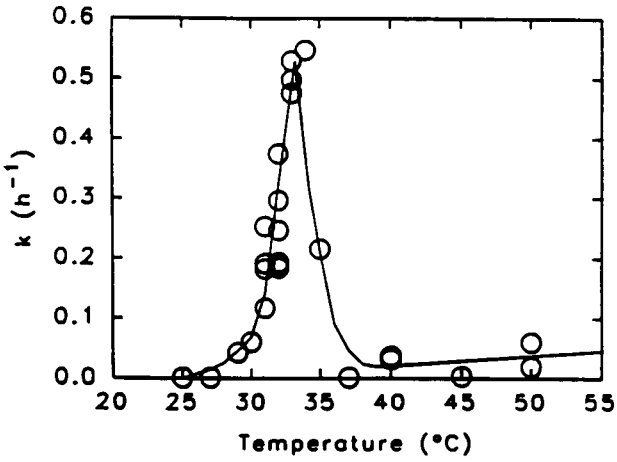

FIGURE 7 Temperature dependence of the permeation of MPE across 50:50 DMPC/DPPC LUV bilayers. Buffer composition: 5 mM MPE, 10 mM NaH_2PO_4/Na_2HPO_4, 40 mM NaCl, 1 mM EDTA, 3.1 mM NaN_3, pH 7.0. The kinetics data were fitted either to a single-exponential decay (membranes in the gel or the liquid-crystalline phase) or to the Laplace transform of normally distributed rate constants (membranes in the mixed-phase state). The permeability rate constants were plotted as a function of the experimental temperatures. The solid line has no theoretical significance and is shown just to guide the eye.

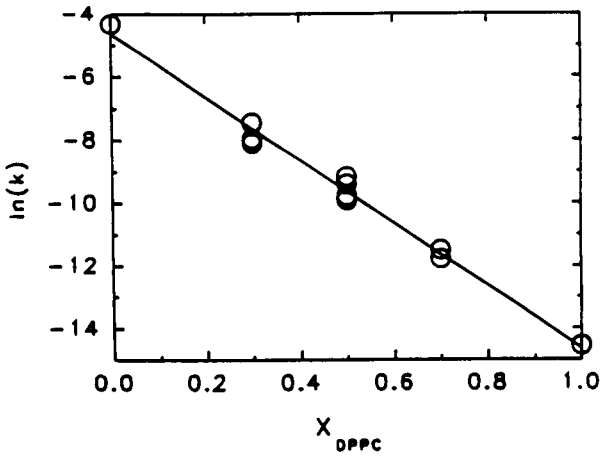

FIGURE 8 Composition dependence of the permeation of MPE across LUV bilayer membranes composed of either DMPC/DPPC mixtures or pure lipids, at the temperature of maximal excess heat capacity. For experimental conditions, see text. Buffer composition: 5 mM MPE, 10 mM NaH_2PO_4/Na_2HPO_4, 40 mM NaCl, 1 mM EDTA, 3.1 mM NaN_3, pH 7.0. The kinetics data were fitted to the Laplace transform of normally distributed rate constants (Eq. A5). The natural logarithm of the average permeability rate constants, k (s^{-1}), were plotted as a function of the DPPC mole fraction, X_{DPPC}. The solid line represents the best fit to a straight line: $\ln(k) = -10.0\ (\pm 0.4) \times X_{DPPC} - 4.7\ (\pm 0.2)$.

bilayer when gel and fluid domains coexist. The phase coexistence also induces an increase in tracer permeation, as shown in Figs. 4 and 5. A possible difference between one- and two-phase bilayers is the boundary between the domains in the phase coexistence region. This suggests that small polar molecules can cross the membrane at the interface between gel and fluid domains at a much faster rate than through the homogeneous phases. The composition of the coexisting gel and fluid domains can be estimated from the phase diagram shown in Fig. 2. For example, in 50:50 DMPC/DPPC bilayers at 32°C, the fluid domains are enriched with DMPC ($X_{DMPC} = 0.4$), whereas the gel domains are enriched with DPPC ($X_{DPPC} = 0.6$). At the domain interface, the lipid composition probably varies within this range of composition ($0.4 < X_{DPPC} < 0.6$) with an average composition $X_{DPPC} = 0.5$. The maximal permeability of the two-phase membrane also depends on the global composition of the bilayer; in DMPC/DPPC mixtures, an increase in the mole fraction of DPPC from 0.3 to 0.5 or from 0.5 to 0.7 produces a decrease of the permeability rate constant of MPE by one order of magnitude (Fig. 8). This observation suggests that fluctuations within vesicles of the lipid composition at the phase interfaces can produce fluctuations in the permeability coefficient of the vesicle bilayer. On the one hand, extruded vesicles 100 nm in diameter are small objects. The volume of one vesicle is $\sim 5 \times 10^{-22}\ m^3$ ($5 \times 10^{-13}\ \mu l$). Thus, the number of trapped solute molecules is also small; vesicles prepared in the presence of 5 mM solute trap an average of 1600 solute molecules per vesicle. The number of trapped radioactive solutes is much lower; under the experimental conditions used in this study, a vesicle contains at most 10 labeled molecules. On the other hand, the number of vesicles in suspension is large; 1 ml of a 10 mM phospholipid suspension contains about 3×10^{13} vesicles. Thus, the permeation of the trapped radioactive solutes across the vesicle bilayers is best characterized by a distribution of rate constants within the vesicle population, $f(k)$.

The efflux kinetics, $F(t)$, is the Laplace transform of $f(k)$ (Hopfer, 1981). The distribution $f(k)$ is not known a priori; if it is assumed that $f(k)$ is a normal (Gaussian) distribution, its Laplace transform can be derived analytically (see Appendix). Alternatively, because the logarithms of the rate constants depend on the composition of the membrane, $f(k)$ equally well can be the normal distribution of the *logarithms* of the rate constants. However, because the Laplace transform of this distribution is difficult to obtain analytically, Eq. A.5, based on normal distributions of rate constants, has been used in this work to fit the experimental efflux kinetics and to determine the average and the SD of the permeability rate constants.[1]

Composition dependence of the permeability rate constants

As shown in Fig. 7, the permeability in the two-phase region is considerably enhanced over that in the single-phase region, reaching a maximum value at the temperature of the heat capacity maximum. Analogous results have been observed in one-component phosphatidylcholine bilayers (Papahadjopoulos et al., 1973; Blok et al., 1975; Marsh et al., 1976; Van Hoogevest et al., 1984; El-Mashak and Tsong, 1985; Georgallas et al., 1987; Bramhall et al., 1987). The data in Fig. 8 show that in pure DMPC and DPPC as well as in DMPC/DPPC mixtures, at the temperature of the maximum excess heat capacity, the logarithms of the average permeability rate constants are linearly correlated with the mole fraction of DPPC in the total system:

$$\ln(k_{X_{DPPC}}) = -10\,X_{DPPC} + \ln(k_{DMPC}) = (1 - X_{DPPC})\ln(k_{DMPC}) + X_{DPPC}\ln(k_{DPPC}). \quad (8)$$

The experimental results show that DMPC bilayers are more permeable than DPPC bilayers, with the ratio of the permeability rate constants for pure DMPC and pure DPPC bilayers equal to 2×10^4. The rather surprising conclusion is that, at the excess heat capacity maximum, $\ln(k)$ is a simple system mole fraction weighted average of the values of $\ln(k)$ for the pure components. In the two-phase coexistence region, the bulk of the system has either the composition of the solid or the fluid phase. The portion of the system at the solid-fluid interface, however, on average has the composition of the total system. In this case, $X_{DPPC} = 0.50$. The simplest explanation for the result expressed in Eq. 8 is that the excess permeability in the two-phase region is associated

[1] The mean rate constants can be evaluated from the area under the efflux curve (Heimburg and Marsh, 1993). This method of calculation gives rate constants that are consistently 22% lower that those calculated from the Laplace transform. We have no explanation for this discrepancy.

with the solid-fluid interface and that it is a simple average of the excess permeabilities of the solid-fluid interfaces in the single-component DMPC and DPPC bilayers.

The apparent fraction of lipids at the interface between phases

In one-component systems, the sharp maximum in solute permeability in the two-phase coexistence region has been attributed either to fluctuations in the lateral compressibility of the bilayers at T_m (Linden et al., 1973; Doniach, 1978; Nagle and Scott, 1978; Georgallas et al., 1987) or to a property of the interfacial region between solid and fluid phases (Papahadjopoulos et al., 1973; Marsh et al., 1976; Kanehisa and Tsong, 1978; Van Hoogevest et al., 1984). Monte Carlo calculations show that the permeability increase in the two-phase region for one-component systems to be correlated with the fraction of interfacial lipids (Cruzeiro-Hansson and Mouritsen, 1988; Ipsen et al., 1990).

The argument in the preceding section supports the idea that the permeability in the two-component, two-phase bilayer is a property of the solid-fluid interface. Is the permeability function for the 50:50 mixture shown in Fig. 7 correlated with the fraction of interface lipid? It is not possible to answer this question in a straightforward way, because no theory exists for determining the fraction of lipid in the interface, F_{fg}. In an ideal binary lipid mixture, it is reasonable to expect the fraction of lipid at the interface between gel and fluid phases to be a maximum when the fractions of gel and fluid phases are equal. This condition coincides approximately with the maximum in the excess heat capacity function, if the heat of melting of the two components are equal. For DMPC/DPPC mixtures, Von Dreele (1978) showed that the nonideality parameters for the 50:50 mixture for both gel and fluid phases are close to 1.0, the ideal value, but with nonideality in the gel phase being greater than that in the fluid phase. Under these conditions, it seems reasonable to expect that the maximum fraction of interfacial lipid in this system occurs close to the maximum in the excess heat capacity curve. As can be seen by comparing Figs. 3 *B* and 7, the temperature of the maximum in the excess heat capacity correlates with the temperature of the maximum in the excess permeability. In fact, as shown in Fig. 10, *B* and *C*, the excess heat capacity values correlate with the permeability coefficients and with their natural logarithms, i.e., the permeability correlates with the variance of the system. It is of interest that application of the theoretical treatment developed by Freire and Biltonen (1978) for one-component systems to the calorimetric data in Fig. 3 for the two-component system yields apparent values of F_{fg}, shown in Fig. 9, that correlate very well with $\ln(k)$, as shown in Fig. 10 *A*. In fact, as noted in the legend of Fig. 10, the correlation with F_{fg} is substantially better than are those shown in Fig. 10, *B* and *C*. Although it is clear that this theoretical treatment is not strictly correct, the correlation of the apparent F_{fg} with $\ln(k)$ is very suggestive.

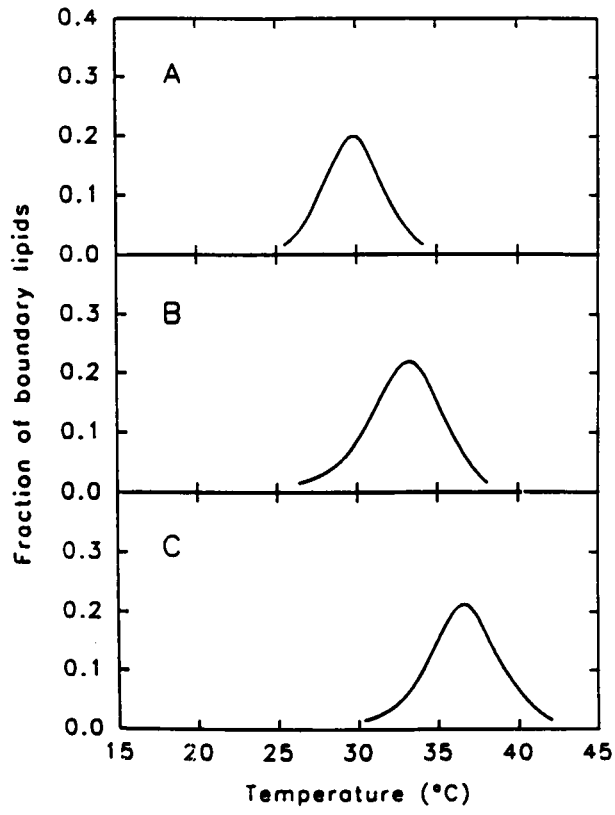

FIGURE 9 Fraction of phospholipid molecules at the gel-fluid boundary, F_{fg}, in DMPC/DPPC vesicles, deduced from the excess heat capacity curves using Eq. 4. (*A*) $X_{DPPC} = 0.3$; (*B*) $X_{DPPC} = 0.5$; (*C*) $X_{DPPC} = 0.7$.

On the basis of the data presented in this paper, we suggest that the excess permeability of MPE observed in DMPC/DPPC two-phase bilayers is localized in the interface between solid and fluid domains. The permeation of solute across lipid bilayers has been modeled as diffusion in nonporous polymers. The diffusion of permeant molecules can then be calculated using the free-volume theory (Lieb and Stein, 1969). Thermal fluctuations generate transient volume defects in the acyl chain region; these pockets of free volume are distributed and create transient holes of different sizes. In this model, the diffusion coefficient is proportional to the frequency of hole formation, ν, and to the probability of a given hole being larger than the permeant molecule, $P(V)$. The probability of finding a hole equal to or larger than the volume V is given by: $P(V) = \exp(-V/V_f)$, where V_f is the average free volume (Cohen and Turnbull, 1959). Therefore, the permeability rate constant can be written as: $k\alpha\nu \exp(-V/V_f)$. In this context, the excess permeability in the two-phase bilayer is due to large density fluctuations in the interface that generate transient excess volume defects. The permeant molecules can diffuse across the bilayer by jumping from a pocket of free volume in the *cis* to a similar pocket in the *trans* monolayer. The ratio of the excess hole volume in the interface, which is equal to or larger than the molecular volume of MPE, to the average excess free volume in the interface is dependent on the average composition of the interface. In one-component bilayers, the Monte Carlo

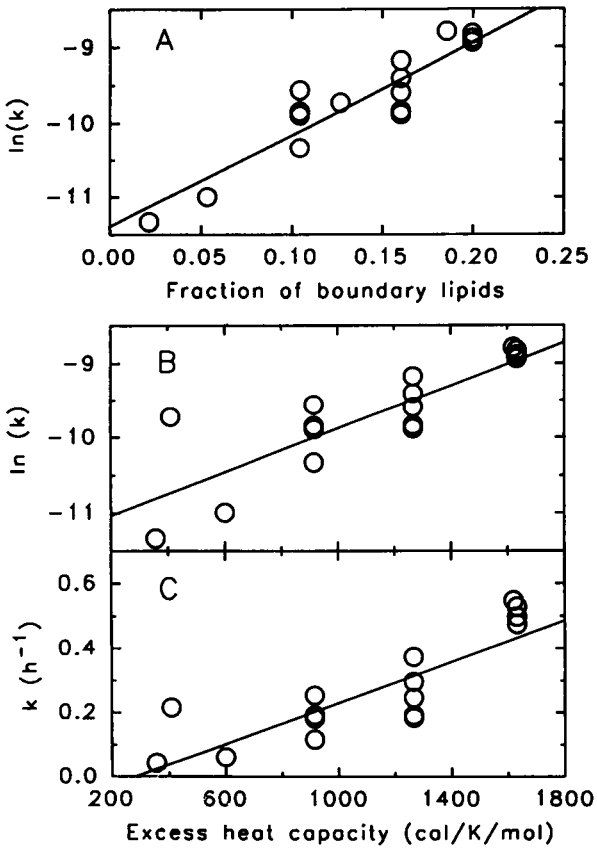

FIGURE 10 (*A*) Correlation between the ln(k) of the MPE permeation rate constants, k (s^{-1}), and the fraction of phospholipid molecules at the gel-fluid boundary, F_{fg}, estimated from the heat capacity curves, in 50:50 DMPC/DPPC LUV at temperatures at which the gel and the liquid-crystalline phases coexist (see Fig. 3). The solid line represents the best fit to a straight line: $\ln(k) = 12.29 \times F_{fg} - 11.40$, correlation coefficient 0.8299. (*B*) Correlation between ln(k) and the excess heat capacity for the same system. The solid line is the best fit to a straight line: $\ln(k) = 0.001446 \times Cp - 11.32$, correlation coefficient 0.6926. (*C*) Correlation between k (h^{-1}) and the excess heat capacity for the same system. The solid line is the best fit to a a straight line: $k = 0.0003206 \times Cp - 0.09085$, correlation coefficient 0.6819. For experimental conditions, see text. Buffer composition: 5 mM MPE, 10 mM NaH_2PO_4/Na_2HPO_4, 40 mM NaCl, 1 mM EDTA, 3.1 mM NaN_3, pH 7.0.

simulations at the phase transition temperature show a decrease in the lateral density fluctuations as the acyl chain length is increased (Ipsen et al., 1990). We suggest that the rate of hole formation and the average free volume also depend on the *average* length of the lipid acyl chains. Previous theoretical models of the bilayer permeability assume a linear relationship between the permeation rate constant and the fraction of interfacial lipids (Kanehisa and Tsong, 1978; Cruzeiro-Hansson and Mouritsen, 1988), i.e., that the membrane permeability is proportional to the area occupied by the interfacial lipids and that the boundary regions have a constant permeability coefficient per unit area. However, the experimental data presented in this article suggest that the permeation rate depends *exponentially* on the fraction of interfacial lipids.

Passive permeability in biological membranes

Although the passage across biological membranes of most solute molecules involves carriers and channel proteins, when the activity of these proteins is inhibited by chemical reagents, the permeability may not be blocked completely. For example, sulfhydryl (SH) reagents, such as *p*-chloromercuribenzoate or *p*-chloromercuribenzene sulfonate, block the water channels of the erythrocyte plasma membrane, but only 50–70% of the water diffusion is inhibited; the residual passive water diffusion is thought to represent the basal diffusive permeability of the lipid bilayer (Brahm, 1982; Pitterich and Lawaczeck, 1985; Benga et al., 1989; Ye and Verkman, 1989). Simple permeation across the lysosomal membrane may also contribute significantly to the translocation of pentoses, amino acids, and dipeptides (for review, see Forster and Lloyd, 1988). Therefore, passive permeation of small polar molecules across phospholipid bilayers can be biologically important, and the investigation of the physicochemical properties of the lipid bilayer itself can lead to the rationalization of biomembrane properties. In this study, we have examined the unusually high permeability to small water-soluble molecules of lipid bilayers, in which two phases coexist at equilibrium, and we have shown that this high permeability, in all probability, is related to density fluctuations in the boundary regions between the coexistent phases. There have been many studies that suggest that in some biological membranes the lipid bilayer exhibits a multiphasic character (Glaser, 1993). If this is the case, then the basal diffusion permeability of the membrane bilayer to solutes could be regulated by the cell through control of this phase structure by biochemical manipulation of lipid composition.

The authors thank Drs. Rodney Biltonen and Derek Marsh for helpful suggestions and criticism.

APPENDIX

Transport kinetics in a population of membrane vesicles

The theory of transport across a membrane has been described on the basis of the thermodynamics of irreversible processes (Kedem and Katchalsky, 1958). However, the transmembrane diffusion of a labeled solute under equilibrium conditions can be analyzed in a much simpler theoretical framework using Fick's first law of diffusion.

For a single membrane vesicle, the fractional entrapment, $F(t)$, i.e., the amount of labeled solute associated with the vesicle, will exponentially decrease as

$$F(t) = \frac{q_t - q_\infty}{q_0 - q_\infty} = \exp(-kt), \tag{A1}$$

where q_0, q_t, and q_∞ are the amounts of labeled solute in the vesicle at the beginning of the experiment ($t = 0$), at time t, and at equilibrium ($t = \infty$), respectively; k is the permeability rate constant defined as

$$k = P\frac{A}{V}, \tag{A2}$$

where P is the phenomenological permeability coefficient, A is the area of the mid-bilayer surface of the vesicle, and V is the volume of the vesicle.

For a population of vesicles, the total fractional entrapment is the sum of the fractional entrapment of each individual vesicle (Hopfer, 1981):

$$F(t) = \sum_{i=0}^{N} f_i F_i(t) = \sum_{i=0}^{N} f_i \exp(-k_i t), \quad \text{(A3)}$$

where N is the total number of vesicles, f_i is the relative contribution, F_i the fractional entrapment, and k_i the permeability rate constant of vesicle i. If all of the vesicles are identical with respect to the membrane properties and geometry, then the permeability rate constant is the same for each vesicle, $k_i = k$, and the contribution of each vesicle is the same, $f_i = 1/N$. Thus, the kinetics of solute permeability in a population of homogeneous vesicles is identical to that of a single vesicle, a single-exponential decay.

In standard permeability experiments, the number of vesicles in suspension is very large; there are on the order of 10^{13} vesicles of 100 nm diameter in 1 ml of vesicle suspension at a phospholipid concentration of 10 mM. Therefore, the summation in Eq. A.3 can be written as an integration:

$$F(t) = \int_0^{\infty} f(k) \exp(-kt)\, dk \quad \text{(A4)}$$

This equation is the Laplace transform by which $f(k)$, the distribution of the rate constants k, is transformed into $F(t)$, the fractional entrapment kinetics. The Laplace transform of the normal distribution with a mean, μ, and a SD, σ, can be derived from published tables of the Laplace transform (Kaplan, 1962; Doetsch, 1971):

$$F(t) = \frac{1}{2} \exp\left(\frac{\sigma^2}{2} t^2 - \mu t\right) \operatorname{erfc}\left[\frac{\sigma}{\sqrt{2}}\left(t - \frac{\mu}{\sigma^2}\right)\right], \quad \text{(A5)}$$

where erfc is the complementary error function. Note that if the distribution is narrow ($\sigma \to 0$), then the distribution of the rate constants becomes almost discrete, and the vesicle population has the same permeability kinetics as a homogeneous population.

REFERENCES

Bartlett, G. R. 1959. Phosphorous assay in column chromatography. *J. Biol. Chem.* 234:466–468.

Benga, G., O. Popescu, V. Borza, V. I. Pop, and A. Hodârnu. 1989. Water exchange through erythrocyte membranes: biochemical and nuclear magnetic resonance studies reevaluating the effects of sulfhydryl reagents and of proteolytic enzymes on human membranes. *J. Membr. Biol.* 108:105–113.

Blok, M. C., E. C. Van der Neut-Kok, L. L. Van Deenen, and J. De Gier. 1975. The effect of chain length and lipid phase transitions on the selective permeability properties of liposomes. *Biochim. Biophys. Acta.* 406:187–196.

Brahm, J. 1982. Diffusional water permeability of human erythrocytes and their ghosts. *J. Gen. Physiol.* 79:791–819.

Bramhall, J., J. Hofmann, R. DeGuzman, S. Montestruque, and R. Schell. 1987. Temperature dependence of membrane ion conductance analyzed by using the amphiphilic anion 5/6-carboxyfluorescein. *Biochemistry.* 26:6330–6340.

Cohen, M. H., and D. Turnbull. 1959. Molecular transport in liquids and glasses. *J. Chem. Phys.* 31:1164–1169.

Cruzeiro-Hansson, L., and O. G. Mouritsen. 1988. Passive ion permeability of lipid membranes modelled via lipid-domain interfacial area. *Biochim. Biophys. Acta.* 944:63–72.

Doetsch, G. 1971. Guide to the Applications of the Laplace and Z-Transforms, 2nd ed. Van Nostran-Reinhold, New York. 240 pp.

Doniach, S. 1978. Thermodynamic fluctuations in phospholipid bilayers. *J. Chem. Phys.* 68:4912–4916.

Eibl, H. 1978. Phospholipid synthesis: oxazaphospholanes and dioxaphospholanes as intermediates. *Proc. Natl. Acad. Sci. USA.* 75:4074–4077.

El-Mashak, E. M., and T. Y. Tsong. 1985. Ion selectivity of temperature-induced and electric field induced pores in dipalmitoylphosphatidylcholine vesicles. *Biochemistry.* 24:2884–2888.

Forster, S., and J. B. Lloyd. 1988. Solute translocation across the mammalian lysosome membrane. *Biochim. Biophys. Acta.* 947:465–491.

Freire, E., and R. Biltonen. 1978. Estimation of molecular averages and equilibrium fluctuations in lipid bilayer systems from the excess heat capacity function. *Biochim. Biophys. Acta.* 514:54–68.

Georgallas, A., J. D. McArthur, X. P. Ma, C. V. Nguyen, G. R. Palmer, M. A. Singer, and M. Y. Tse. 1987. The diffusion of small ions through phospholipid bilayers. *J. Chem. Phys.* 86:7218–7226.

Glaser, M. 1993. Lipid domains in biological membranes. *Curr. Opin. Struct. Biol.* 3:475–481.

Heimburg, T., and D. Marsh. 1993. Investigation of the secondary and tertiary structural changes of cytochrome *c* in complexes with anionic lipids using amide hydrogen exchange measurements: an FTIR study. *Biophys. J.* 65:2408–2417.

Hope, M. J., M. B. Bally, G. Webb, and P. R. Cullis. 1985. Production of large unilamellar vesicles by a rapid extrusion procedure. Characterization of the size distribution, trapped volume and ability to maintain a membrane potential. *Biochim. Biophys. Acta.* 812:55–65.

Hopfer, U. 1981. Kinetic criteria for carrier-mediated transport mechanisms in membrane vesicles. *Fed. Proc.* 40:2480–2485.

Ipsen, J. H., K. Jørgensen, and O. G. Mouritsen. 1990. Density fluctuations in saturated phospholipid bilayers increase as the acyl-chain length decreases. *Biophys. J.* 58:1099–1107.

Kanehisa, M. I., and T. Y. Tsong. 1978. Cluster model of lipid phase transitions with application to passive permeation of molecules and structure relaxations in lipid bilayers. *J. Am. Chem. Soc.* 100:424–432.

Kaplan, W. 1962. Operational Methods for Linear Systems. Addison-Wesley, Reading, MA. 577 pp.

Kedem, O., and A. Katchalsky. 1958. Thermodynamic analysis of the permeability of biological membranes to non-electrolytes. *Biochim. Biophys. Acta.* 27:229–246.

Lieb, W. R., and W. D. Stein. 1969. Biological membranes behave as nonporous polymeric sheets with respect to the diffusion of non-electrolytes. *Nature.* 224:240–243.

Linden, C. D., K. L. Wright, H. M. McConnell, and C. F. Fox. 1973. Lateral phase separations in membrane lipids and the mechanism of sugar transport in *Escherichia coli*. *Proc. Natl. Acad. Sci. USA.* 70:2271–2275.

Mabrey, S., and J. M. Sturtevant. 1976. Investigation of phase transitions in lipids and lipid mixtures by high sensitivity differential scanning calorimetry. *Proc. Natl. Acad. Sci. USA.* 73:3862–3866.

Marsh, D., A. Watts, and P. F. Knowles. 1976. Evidence of phase boundary lipids. Permeability of tempo-choline into dimyristoyl phosphatidylcholine vesicles at the phase temperature. *Biochim. Biophys. Acta.* 858:161–168.

Nagle, J. F., and H. L. Scott. 1978. Lateral compressibility of lipid mono- and bilayers. Theory of membrane permeability. *Biochim. Biophys. Acta.* 513:236–243.

Papahadjopoulos, D., K. Jacobson, S. Nir, and T. Isac. 1973. Phase transitions in phospholipid vesicles. Fluorescence polarization and permeability measurements concerning the effect of temperature and cholesterol. *Biochim. Biophys. Acta.* 311:330–348.

Pitterich, H., and R. Lawaczeck. 1985. On the water and proton permeabilities across membranes from erythrocyte ghosts. *Biochim. Biophys. Acta.* 821:233–242.

Press, W. H., B. P. Flannery, S. A. Teukolsky, and W. T. Vetterling. 1986. Numerical Recipes. The Art of Scientific Computing. Cambridge University Press, New York. 818 pp.

Stewart, J. C. M. 1980. Colorimetric determination of phospholipids with ammonium ferrothiocyanate. *Anal. Biochem.* 104:10–14.

Van Hoogevest, P., J. De Gier, and B. De Kruijff. 1984. Determination of the size of the packing defects in dimyristoyl phosphatidylcholine bilayers, present at the phase transition temperature. *FEBS Lett.* 171:160–164.

Van Osdol, W. W., M. L. Johnson, Q. Ye, and R. Biltonen. 1991. Relaxation dynamics of the gel to liquid-crystalline transition of phosphatidylcholine bilayers. Effects of chain length and vesicle size. *Biophys. J.* 59:775–785.

Von Dreele, P. H. 1978. Estimation of lateral species separation from phase transitions in nonideal two-dimensional lipid mixtures. *Biochemistry.* 17: 3939–3943.

Wimley, W. C., and T. E. Thompson. 1990. Exchange and flip-flop of dimyristoyl phosphatidylcholine in liquid-crystalline, gel, and two-component, two-phase large unilamellar vesicles. *Biochemistry.* 29:1296–1303.

Ye, R., and A. S. Verkman. 1989. Simultaneous optical measurement of osmotic and diffusional water permeability in cells and liposomes. *Biochemistry.* 28:824–829.